



Bacterial inactivation with iron citrate complex: A new source of dissolved iron in solar photo-Fenton process at near-neutral and alkaline pH



Cristina Ruales-Lonfat^a, José Fernando Barona^b, Andrzej Sienkiewicz^{c,d}, Julia Vélez^a, Luis Norberto Benítez^b, César Pulgarín^{a,*}

^a SB, ISIC, GPAO, Station 6, Ecole Polytechnique Fédérale de Lausanne, 1015 Lausanne, Switzerland

^b Universidad del Valle, Grupo de Investigación en Procesos Avanzados de Oxidación (GAOX), Cali AA. 25360, Colombia

^c SB, IPMC, LPMC, Station 3, Ecole Polytechnique Fédérale de Lausanne, 1015 Lausanne, Switzerland

^d ADSresonances, 1028, Préverenges, Switzerland

ARTICLE INFO

Article history:

Received 4 March 2015

Received in revised form 9 June 2015

Accepted 16 June 2015

Available online 28 June 2015

Keywords:

Iron-citrate complex

Bacterial inactivation

Homogeneous photo-Fenton process

Photo-Fenton at near-neutral and alkaline pH

ABSTRACT

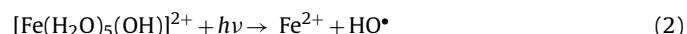
This study reports the first application of Fe-citrate-based photo-Fenton chemistry for the inactivation of *Escherichia coli*. Promising results of bacterial inactivation at near-neutral and alkaline pH conditions were obtained, while using low iron concentration (Fe-citrate concentration: 0.6 mg/L, relative to the Fe content) and avoiding precipitation of ferric hydroxides. The effects of the solution pH and Fe-citrate complex concentration on *E. coli* inactivation during the photo-Fenton reaction were investigated. The efficiency of the homogeneous photo-Fenton process using Fe-citrate complex as a source of iron strongly improved bacterial inactivation as compared with the heterogeneous photo-Fenton treatment (FeSO₄ and goethite as sources of iron) at near-neutral pH. The bacterial inactivation rate increased in the order of goethite < FeSO₄ < Fe-citrate, which agreed well with the trend for the HO[•] radical formation, monitored by ESR. Encouraging results were also obtained while applying this treatment for bacterial inactivation in natural water samples from Lake Geneva (Switzerland) at pH 8.5, since no bacterial reactivation and/or growth were observed after photo-Fenton treatment. This type of application is promising, considering the simplicity of the installations and procedures, the ability to use the Sun as the light source, and the safety of all of the chemicals in this system.

© 2015 Elsevier B.V. All rights reserved.

1. Introduction

The photo-assisted Fenton system is one of the most popular and widely studied advanced oxidation processes (AOPs). Its oxidative action is a result of the formation of reactive oxygen species (ROS), especially hydroxyl radicals, HO[•], following the oxidation of ferrous iron by hydrogen peroxide (Eq. (1)). Ferrous iron, in the absence of any other complexing agents, has the tendency to rapidly get oxidized and form different aqua-Fe³⁺ species, depending on the pH levels of the medium. At low pH (~2.8), it tends to form [Fe(H₂O)₅(OH)]²⁺, which exhibits significant photoactivity in the UV-visible(UV-Vis) part of the solar spectrum and allows for the regeneration of Fe²⁺, when illuminated by solar radiation (Eq. (2)) [1,2]. The regenerated Fe²⁺ reacts again with H₂O₂, thus,

continuing the formation of HO[•] radicals in the process known as photo-Fenton.

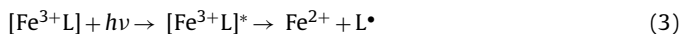


Despite its dual advantages of being economic and environmental friendly, the photo-Fenton reaction has not been widely used in microbial disinfection, due to the theoretical requirement of acidic conditions. However, from the seminal paper of Rincón and Pulgarín [3] interest has grown over the past few years, in the application of near-neutral photo-Fenton treatment for water and wastewater disinfection [4–11]. In the absence of iron ligands, at near-neutral pH, a spontaneous chemical oxidation of Fe²⁺ to Fe³⁺ by dissolved oxygen in water occurs, involving formation of ferric (hydr) oxides, like Fe₂O₃·nH₂O [12], which do not re-dissolve in water, thus, inhibiting the recycling in solution of Fe³⁺ back to Fe²⁺. However, soluble iron in the mg/L range was detected at pH 6.5 in the presence of bacteria, due to siderophores secreted by bacteria

* Corresponding author. Fax: +41 21 693 6161.

E-mail address: Cesar.pulgarin@epfl.ch (C. Pulgarín).

and by-products generated from the degradation of bacterial components [10]. So for the use of iron-chelating agents are exclusively being considered for organic pollutants degradation. The resulting iron complexes maintain $\text{Fe}^{3+}/\text{Fe}^{2+}$ solubility at a wide pH range and exhibit high absorbance in the UV-vis region, which allows for using a considerable portion of the solar spectrum, thus, reducing the operating costs. Iron complexes are photochemically reactive via participation in ligand-to-metal charge-transfer (LMCT) transitions (Eq. (3)) [13–15]. Therefore, soluble Fe^{2+} can participate in homogeneous Fenton reaction and thus, enhance the production of hydroxyl radicals (Eq. (1)).



Several Fe^{3+} chelates have been evaluated for oxidation of hydrogen peroxide at circumneutral pH [16]. However, the harmful effects of some chelating agents, such as ethylenediaminetetraacetic acid (EDTA) and nitrilotriacetic acid, have recently been acknowledged, and their use in environmental applications and especially in drinking water disinfection has been avoided. Many other low molecular weight organic compounds (e.g. oxalate, citrate, malonate) were used as model organic ligands in numerous studies, showing that photochemical reactions of their complexes with Fe^{3+} were potentially important sources of Fe^{2+} , $\text{O}_2^\bullet-//\text{HO}_2^\bullet$, H_2O_2 and HO^\bullet in illuminated surface waters [15,17–19].

Ferric–citrate complex is a good alternative for iron solubilization in the photo-Fenton processes. Although its photolysis shows a lower quantum yield for Fe^{2+} generation than that observed for ferrioxalate, citrate is less toxic [13,20,21], has higher cumulative stabilization constants ($\log \beta = 14.29$) [22], is readily available and can be used at higher pH values than oxalate (up to pH 9.0) [23]. Ferric–citrate complexes have been successfully implemented for the photo-Fenton treatment at near-neutral pH conditions and with using artificial or solar light towards degradation of organic compounds in polluted waters [13,14,24–26]. However, there has been no report on the application of this system as a disinfection technology.

In this work, the influence of the pH (6.5, 7.5 and 8.5) on the photo-degradation of Fe–citrate complex and on the generation of ROS during Fe–citrate-based photo-Fenton process was assessed. The aim of this research was to study the disinfection ability of the Fe–citrate complex in photo-Fenton treatment under simulated solar light illumination, at near-neutral and alkaline pH in water. The effects of the solution pH and Fe–citrate complex concentration on *Escherichia coli* inactivation during the photo-Fenton reaction were investigated. Furthermore, bacterial inactivation by photo-Fenton process mediated by Fe–citrate complex, FeSO_4 and goethite at near-neutral pH were comparatively studied to evaluate homogeneous and heterogeneous contributions to the *E. coli* inactivation mechanism and the disinfecting ability of these systems were evaluated quantitatively.

Finally, the efficiency of Fe–citrate-based photo-Fenton process was also demonstrated in real-world condition, i.e. in natural water samples from Lake Geneva (Switzerland) at pH 8.5 and containing 108 mg/L of HCO_3^- . The results of this research demonstrate promise of the first applications of Fe–citrate-based photo-Fenton chemistry applied to microbial inactivation under near-neutral and alkaline pH conditions.

2. Materials and methods

2.1. Chemicals

Ferrous sulphate heptahydrate ($\text{FeSO}_4 \cdot 7\text{H}_2\text{O}$) (Riedel-de Haen 99–103.4%); Goethite ($\alpha\text{-FeO(OH)}$), 30–50 mesh (Sigma-Aldrich South Africa); Ferric chloride (FeCl_3) (98% carlo erba), Trisodium cit-

Table 1
Physicochemical characteristics of the waters used in the experiments.

Parameter	Milli-Q water	Lake Geneva water
Conductivity at 20 °C ($\mu\text{S/cm}$)	<0.055	252
Transmittance at 254 nm (%)	100	96
pH	6.5	8.4
Total organic carbon (TOC) (mg C/L)	<0.005	0.8–1
Iron (mg/L)	–	0.019
Phosphates	–	0.012
Hydrogen carbonate (mg HCO_3^- /L)	–	108
Chloride (mg Cl^- /L)	–	8.0
Sulfate (mg SO_4^{2-} /L)	–	48
Nitrate (mg NO_3^- /L)	–	2.7

rate dihydrate ($\text{Na}_3\text{C}_6\text{H}_5\text{O}_7 \cdot 2\text{H}_2\text{O}$) (99% Merck); Sodium hydrogen carbonate (NaHCO_3) (analytical grade, Merck); Hydrogen peroxide (H_2O_2) 30% w/v (Riedel de Haen); Titanium (IV) oxy sulfate (TiOSO_4) (Fluka); Sodium hydroxide (NaOH , 98%) and hydrochloric acid (HCl , 36.5%), were purchased from Sigma-Aldrich. The spin-trap, 5,5-dimethyl-1-pyrroline-N-oxide (DMPO), was purchased from Enzo Life Sciences (ELS) AG (Lausen, Switzerland).

All solutions were prepared immediately prior to irradiation with the use of Milli-Q water (18.2 MΩ-cm). Two different types of water were used to suspend bacteria, i.e. Milli-Q water and the natural water from Lake Geneva. Table 1 shows the physicochemical characteristics of these waters.

2.2. Fe–citrate complex preparation

Fe–citrate complex was prepared according to the modified European patent [27]. Ferric chloride (4.1 g) and sodium hydrogen carbonate (3.0 g) were dispersed in 50 mL of distilled water and dissolved therein by stirring. This solution was degassed under vacuum for 2 h. Then, with constant stirring, Trisodium citrate dihydrate (4.0 g) were added. The colour of the solution turned to a pale brown. The solution was stored in the dark for 24 h. Then, 40 mL of methanol was added to the brown solution under constant stirring at 25 °C and a brown precipitate was formed. The resulting suspension was centrifuged (5 min at 5000 rpm) to remove the precipitate, and the clear supernatant solution was separated by filtration. The precipitate was washed with methanol at least three times and dried under vacuum at room temperature.

2.3. Bacterial strains and growth media

The bacterial strain used was *E. coli* K-12 (MG1655), a non-pathogenic wild-type strain, which can be handled with little genetic manipulation. Bacteria were inoculated from a stock in a nutrient-rich medium, Luria-Bertani (LB) broth, and incubated in a shaker incubator at 37 °C and 180 rpm. After 8 h, cells were diluted (1% v/v) in the pre-heated LB broth and incubated at 37 °C for 15 h in the incubator until a stationary physiological phase was reached. Cells were separated during the stationary growth phase by centrifugation (15 min at 5000 rpm, at 4 °C). The bacterial pellet was re-suspended and washed three times with a saline solution in the centrifuge. This procedure resulted in a bacterial pellet of approximately 10^9 colony forming units per millilitre (CFU/mL).

2.4. Experimental

2.4.1. Photo-degradation of Fe–citrate complex at various pH values

The photo-degradation of Fe–citrate complex in the presence of H_2O_2 at controlled pH levels of 6.5, 7.5 and 8.5 were determined by molecular absorption spectroscopy, using a UV–vis spectrophotometer, Model 1700 (Shimadzu, Japan). Fe–citrate concentration:

3.8 mg/L relative to the Fe content. Hydrogen peroxide concentration: 10 mg/L.

2.4.2. Photo-inactivation experiments

All bacterial inactivation experiments were performed in Pyrex reactors (4 cm × 9 cm, 100 mL). The Pyrex reactors containing the bacterial suspension in water (approximately 10⁶ CFU/mL) were placed in the dark at 25 °C and kept under magnetic stirring for at least 30 min to let the bacteria adapt to the new matrix and to allow the die-off and equilibration of the most stress-sensitive species.

The following systems were analysed for the inactivation effect on *E. coli*. (i) photo-Fenton process mediated by Fe–citrate (Fe–citrate concentration: 0.6 mg/L relative to the Fe content) at various pH values: 6.5, 7.5 and 8.5.; (ii) photo-Fenton process with different Fe–citrate concentrations: 0.1, 0.3, 0.6, 1.0 and 2.0 mg/L, relative to the Fe content; (iii) photo-Fenton process mediated by different iron sources Fe–citrate, FeSO₄, goethite and under control experiments: Fe–citrate/light, Fe–citrate/H₂O₂/dark, light alone and H₂O₂/light, (Fe–citrate concentration: 0.6 mg/L relative to the Fe content) and (iv) photo-Fenton process mediated by Fe–citrate suspended in natural water from lake Geneva (Switzerland). In the experiments, iron was added to a solution of *E. coli*. Then, the pH was adjusted to 6.5 or 7.5 or 8.5, depending on the experiment. Finally, H₂O₂ (10 mg/L) was added to the reactor as the last component. Aliquots were collected during set intervals within the inactivation time.

Solar exposure experiments were carried out using a solar simulator CPS Suntest System (Heraeus Noblelight, Hanau, Germany). The Suntest bears a lamp that emits ~0.5% of the photons at wavelengths <300 nm (UVC cut-off at 290 nm), ~7% between 300 and 400 nm and the rest follow the solar spectrum above that value until IR range (IR was cut-off by filtering). The radiance intensity was measured by a spectroradiometer, Model ILT-900-R (International Light Technologies) and corresponded to 820 W/m² of light global intensity (20.2 W/m² on the UV).

During the experiments, the temperature in the reactors did not exceed 38 °C. After each experiment, the reactors were rinsed with nitric acid (10%) followed by washing with distilled water and, finally, autoclaved. All the experiments were conducted triplicate, with good reproducibility (<10% difference between replicates).

2.4.3. Post-irradiation events

Bacterial reactivation and/or growth were determined for photo-Fenton experiments by keeping the final samples in the dark, at room temperature (20–25 °C) for 24 and 48 h before the measurement of the CFU.

2.5. Analytical methods

Total dissolved iron was measured using an Inductively Coupled Plasma Mass Spectrometer (ICP-MS), Model ICPE-9000 (Shimadzu, Japan). Samples were filtered (0.25 µm) and kept in acid solution prior to the determination. The detection limit ranges of spectrometry used for this experiment were (0.2–0.9 µg/L). The concentration of H₂O₂ was monitored using a titanium (IV) oxysulfate solution via a spectrophotometric method at 410 nm (modified method DIN 38 402H15). The titanium (IV) oxysulfate method has a 0.1 mg/L detection limit. The pH was measured with a pH-metre Metrohm 827 pH-lab using a glass electrode.

2.5.1. Electron spin resonance spectroscopy (ESR)

Electron spin resonance spectroscopy (ESR) in combination with spin-trapping was used to monitor the formation of ROS, i.e. namely hydroxyl (HO•) and superoxide (O₂•⁻) radicals, generated by homogeneous and heterogeneous photo-Fenton processes mediated by Fe–citrate, FeSO₄ and goethite. A stock solution of

DMPO (0.5 M) was prepared in ultrapure water (Milli-Q) and stored at –20 °C.

The following systems were used to study the light-induced ROS formation in photo-Fenton process: (i) Fe–citrate concentration: 3.8 mg/L relative to the Fe content, H₂O₂:10 mg/L; (ii) Fe–citrate or FeSO₄ or goethite concentration: 0.6 mg/L relative to the Fe content and 10 mg/L of H₂O₂. The solutions of system (i) were exposed to UV-A light (~365 nm) using a UV spot light source, Lightingcure™, model LC-8 (Hamamatsu Photonics, France). Systems (ii) were exposed to simulated solar light (global light intensity of 820 W/m² and 20.2 W/m² in the UV-A range) under constant agitation. Just before performing the photo-generation of ROS, DMPO (final concentration of 100 mM) was added to Fenton's reagents. Subsequently, 2 mL aliquots of the prepared samples were transferred into small Pyrex beakers (5 mL volume, 20 mm outer diameter and 30 mm height) and positioned in a solar light simulator, CPS Suntest System (Heraeus Noblelight, Hanau, Germany). Next, at the selected time intervals, the sample of the Fenton's reagents was drawn into thin glass capillaries (0.7 mm ID/0.87 mm OD, from VitroCom, NJ, USA), which were then sealed on both ends using the Cha-Seal™ tube-sealing compound (Medex International, Inc., USA). ESR measurements were carried out at room temperature using a Bruker X-band spectrometer, Model EleXsys 500 (Bruker BioSpin, Karlsruhe, Germany) equipped with a high-Q cylindrical TE₀₁₁ microwave cavity, Model ER4123SHQE. The typical instrumental settings were: frequency of 9.4 GHz; microwave power of 0.63 mW; scan width of 120 G; magnetic field resolution of 2048 points; modulation frequency of 100 kHz; modulation amplitude of 1.0 G; receiver gain of 60 dB; conversion time of 40.96 ms; time constant of 20.48 ms and sweep time of 84 s.

The spin-adducts concentrations were estimated using the double integration of the first-derivative ESR spectra. The actual concentrations of spin-adducts were derived by comparison with a calibrated ESR signal, which was acquired for a stable nitroxide radical, TEMPOL (10 µmol/L). The data analysis was carried out using Origin Pro 9.0 software.

2.6. Data treatment

The bacterial inactivation kinetics can be described by the first order kinetic model proposed by ChickseWatson (Eq. (4)) [28]:

$$N_t = N_0 e^{-kt} \quad (4)$$

where N_0 is the concentration of viable organisms before radiation exposure; N_t is the concentration of organisms surviving after irradiation time; t is the irradiation time (at constant light flux) and k is the first order inactivation rate.

To compare inactivation between the different treatments tested, the constants of inactivation rate were obtained, k_{obs} , from fitting of plots of log(CFU/mL) vs. time. The fitting was carried out by GInaFiT, a tool of Microsoft Excel for testing different types of microbial survival models on experimental data [29]. The root mean square error of the fit to the experimental data was evaluated. The R^2 of the model was in most cases superior to 0.9.

The standard error was calculated by the sample standard deviation divided by the square root of the sample size, as follows: $SE = \frac{S}{\sqrt{n}}$, where S is the sample standard deviation, and n is the size (number of observations) of the sample. The standard deviation was calculated using a minimum of three measures. Standard error was found to be approximately 5%.

3. Results and discussion

3.1. Spectral properties of Fe^{3+} –citrate complex

The UV-vis absorption spectra of trisodium citrate and Fe^{3+} –citrate complex are presented in Fig. 1. Trisodium citrate does not absorb significantly beyond 230 nm. The absorption spectrum of Fe^{3+} –citrate shows a maximum absorption bands at 350 and 490 nm. The difference in the absorption spectra confirmed the formation of metal ions complex by the complexing agent *trisodium citrate*. According to these results, it can be shown that Fe–citrate complexes absorb in the UV-vis region (300–450 nm) and thus, have the potential for utilizing sunlight as an irradiation source.

3.2. Photo-degradation of Fe–citrate complex in the presence of H_2O_2 at different controlled pH levels

Before evaluating the photo-Fenton-mediated bacterial inactivation, control experiments were carried out in order to understand the behaviour of the iron–citrate complex during the photo-Fenton reaction in the absence of bacteria.

The curves of Fe–citrate disappearance kinetics at different controlled pH levels of 6.5, 7.5 and 8.5 (by NaOH addition) upon irradiation with simulated solar light are presented in Fig. 2a. The total disappearance of Fe–citrate complex was observed at different pH values. However, it was markedly accelerated at pH 6.5 and 7.5 (Fig. 2a, traces (\blacktriangle) and (\blacksquare)). At these pH values, citrate forms stable complexes with ferric ions (Fe^{3+}) as can be observed in the conditional stability constants (Fig. 3). The photochemical reactions of these complexes undergo via LMCT, thus, by dissociating into Fe^{2+} and Citrate $^{2-}$ (Eq. (5)) [30]. Thus, the dissociation into citrate ligand is certainly responsible for the significant changes observed in the UV-visible absorption spectra [31]. It is interesting to notice that at pH 8.5, in contrast to pH 6.5 and 7.5, no significant degradation of the Fe–citrate was observed before 60 min of treatment (Fig. 2a, trace (\bullet)) indicating that the Fe–citrate complex was more stable at this pH. These results could be attributed to:

- (i) The possible structural changes of the Fe^{3+} –citrate complexes. In particular, Vukosav et al. [31,32] suggested a bond splitting between citrate hydroxyl oxygen and Fe^{3+} in the iron coor-

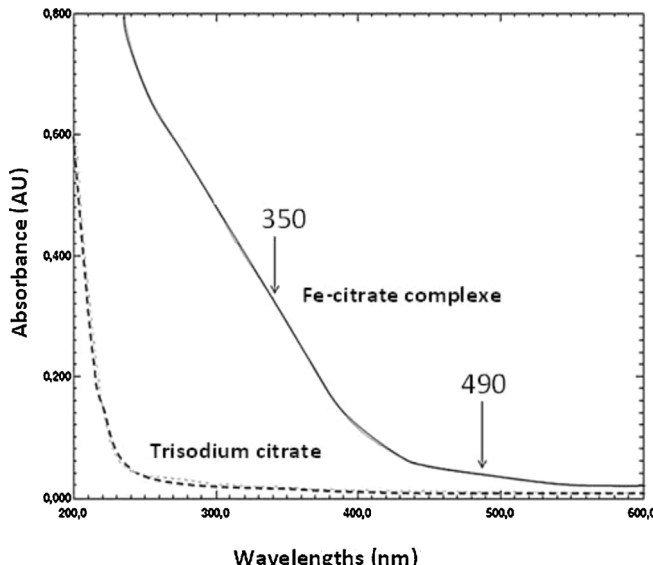


Fig. 1. UV-vis absorption spectra of trisodium citrate (13.3 mg/L) and Fe–citrate synthesized (5.6 mg/L), pH 6.5.

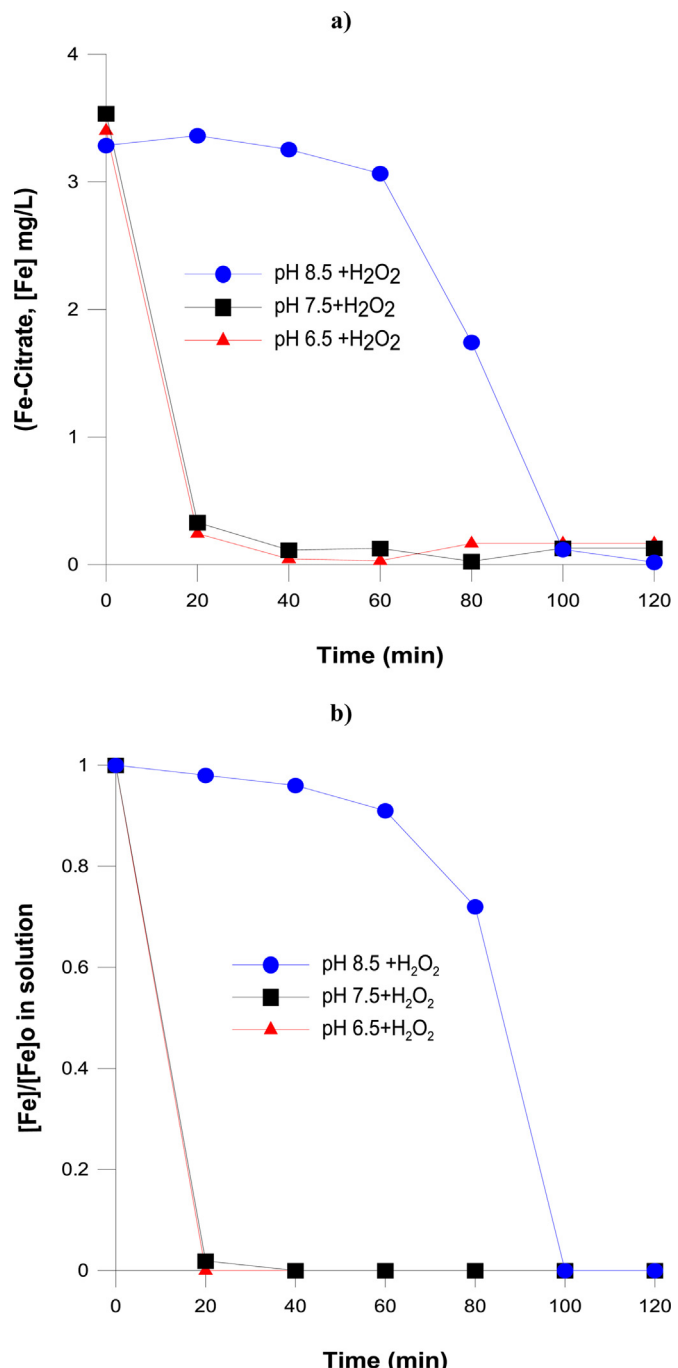


Fig. 2. (a) UV-vis spectra of Fe–citrate; (b) disappearance of Fe–citrate during photo-Fenton reaction; (c) evolution of dissolved iron during photo-Fenton reaction at different controlled pH values: (\blacktriangle) pH 6.5; (\blacksquare) 7.5 and (\bullet) 8.5. Fe–citrate concentration: 3.8 mg/L relative to the Fe content, $[\text{H}_2\text{O}_2]$: 10 mg/L. Irradiated with simulated solar light. Experiments were conducted in triplicate and standard error was found to be approximately 5%. (For interpretation of the references to colour in this figure legend, the reader is referred to the web version of this article.)

- dination sphere above pH 7.0. This change would enable the attachment of OH^- ions from the solution to the coordination sphere of Fe^{3+} –citrate complexes. In the reported experiments, the chemical changes in the complex were evidenced only by voltammetric measurements, being, however, unlikely to be detected by UV-vis spectrophotometry.
- (ii) The presence of $\text{Fe}^{3+}/\text{Fe}^{2+}$ mixed-valence complexes which may occur at high pH [33]. The two mixed-valence complexes, $\text{Fe}^{3+}\text{Fe}^{2+}\text{Cit}^{2+}$ and $\text{Fe}^{3+}\text{Fe}^{2+}\text{Cit}_2\text{H}_2^+$, have been previously iden-

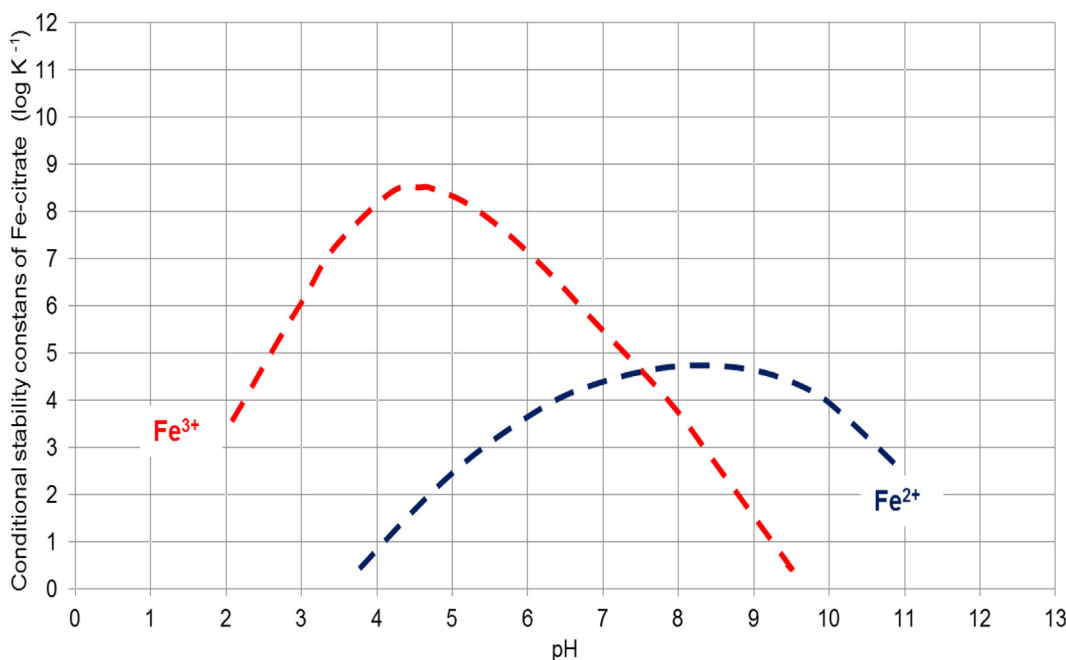
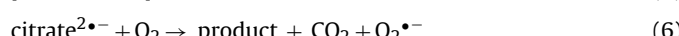


Fig. 3. Conditional stability constants for iron with citric acid.

tified in aqueous citrate media from spectrophotometric absorption data [34].

- (iii) Photo-generated ferrous iron-mediated ferric–ferrous ion exchange in the Fe^{3+} –citrate complex. According to the stability constants conditional of Fe–citrate ($\log K'$) (Fig. 3), the Fe^{2+} –citrate complex becomes the predominant complex at pH above 7.5 [35]. Krishnamurti and Huang [36] have reported that citrate form a stable complex with Fe^{2+} that considerably retarded its oxidation at constant pH 6.0. A similar finding using fulvic acid have reported by Rey et al. [35]. They observed that Fe^{2+} –fulvic acid complexes are formed at basic pH and increasing the pH results in a strong decrease in the rate constants for the dissociation of Fe^{2+} –fulvic acid complexes. Pham and Waite [37] have also supports the presence of Fe^{2+} –citrate species at near-neutral and alkaline solutions. Other studies indicate that Fe^{2+} in a complexed form (FeL^{2+}), is stable with respect to oxidation and such ligand stabilization has been suggested as an explanation for the apparent presence of Fe^{2+} in oxic solutions that contain relatively high levels of organic matter.

A good correlation between the photo-decomposition of the Fe–citrate complex with the precipitation of iron in the system at pH 6.5, 7.5 and 8.5 was found (Fig. 2a and b). The iron precipitation at pH 6.5 and 7.5 before 20 min of reaction (traces (▲) and (■)) is due to the oxidative degradation of the citrate ligand (Eq. (6)) [30]. Thus, in the absence of citrate ligand and at near-neutral pH, a spontaneous chemical oxidation of Fe^{2+} ions to Fe^{3+} occurs by both dissolved oxygen in the aqueous solution and added H_2O_2 . The subsequent hydrolysis leads to the formation of the ferric hydroxocomplex ($Fe(OH)_2^{+}$) (Eq. (7)). These iron intermediates ultimately transform into stable iron oxide end-products, such as goethite or lepidocrocite [38]. In contrast, in the experiments conducted at pH 8.5, dissolved iron was observed up to 60 min of reaction and began to precipitate when the Fe–citrate complex started to be degraded.



In our experiments, photo-products formed from the photo-dissociation of Fe–citrate did not contribute to solubilization of iron, contrary to the findings by Abida et al. [39], who observed the stabilization of dissolved Fe^{2+} concentration at pH 6.0 after 120 min of irradiation.

The results of Fig. 1(a and b) show that the stability of Fe–citrate complex in the presence of H_2O_2 under simulated solar light is several times higher at pH 8.5 than at pH 6.5 and 7.5 and its photo-decay rates follow the order: $6.5 \approx 7.5 > 8.5$. In fact, previous work reported that oxalate was the best choice as ligand in acidic solutions and that citrate was preferable in neutral aqueous media for photo-Fenton studies [14]. Therefore, citrate proved to be a good ligand for iron ions to be used at near-neutral and alkaline pH for photo-Fenton studies.

3.3. ROS generation during Fe–citrate-based photo-Fenton system at various pH values

The photo-generation of ROS, i.e. HO^\bullet and $O_2\bullet^-$ in the aqueous solution was determined during the Fe–citrate-based photo-Fenton process at pH 6.5, 7.5 and 8.5. The ESR spin-trapping technique, with DMPO as a spin trap was employed to identify both HO^\bullet and $O_2\bullet^-$ radicals, thus, leading to the formation of spin-adducts, DMPO-OH or DMPO-OOH, respectively. Both resulting paramagnetic products reveal distinct and easily recognizable ESR spectra. However, the DMPO-OOH spin adduct is well known to be highly unstable and rapidly decomposing into the DMPO-OH spin adduct [40].

Fig. 4 shows that pH value has a great effect on the photo-generation of HO^\bullet radicals. The photo-Fenton treatment at pH 8.5 (trace (●)) showed higher generation of HO^\bullet radicals, as compared with the same system at pH 7.5 and 6.5 with 1.7, 1.0 and 0.9 mmol of HO^\bullet radical, respectively (traces (■) and (▲)). It is due to the mayor stability of the Fe–citrate complex at pH 8.5 as was showed in Fig. 2a and b, trace (●), enhancing Fenton reaction and the HO^\bullet production rate (Eq. (10)).

According to Chen et al. [30], the stability of Fe^{3+}/Fe^{2+} –citrate was a predominant factor for the pH-dependent generation of HO in the Fe–citrate solutions. The main Fe–citrate species with fer-

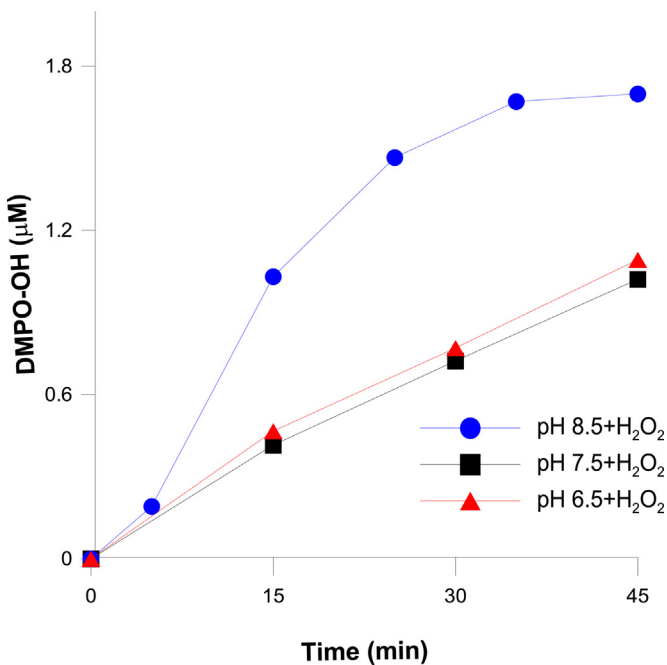
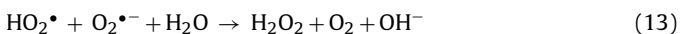
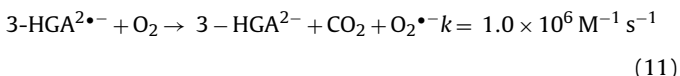
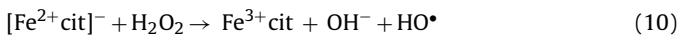
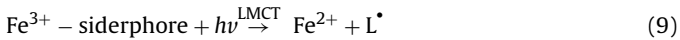
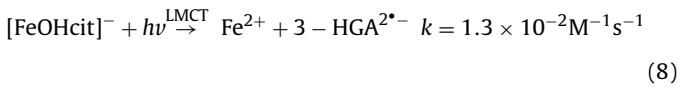


Fig. 4. The ESR-measured formation of hydroxyl radical (HO^\bullet) during photo-Fenton process mediated by Fe-citrate at different pH values: (\blacktriangle) pH 6.5; (\blacksquare) 7.5 and (\bullet) 8.5. Fe-citrate concentration: 3.8 mg/L relative to the Fe content, $[\text{H}_2\text{O}_2]$: 10 mg/L. Irradiated with UV-A radiation. (For interpretation of the references to colour in this figure legend, the reader is referred to the web version of this article.)

rous and ferric iron ions include $[\text{FeHcit}]$, $[\text{Fecit}]^-$, $[\text{Fecit}]^{2-}$ and $[\text{FeHcit}]^+$, $[\text{Fecit}]$, $[\text{FeOHcit}]^-$, respectively [41]. However, there are some discrepancies in literature concerning the Fe^{3+} -citrate species dominant in solution at different pH values [33,42].

The generation of HO radicals is induced by photoactive $[\text{FeOHcit}]^-$ complex, which is the main species formed at neutral pH [14,30] and can presumably be interpreted according to the following reactions (Eqs. (7)–(13)).



It has been well-established that the mechanism of photo-generation of HO^\bullet radicals is generated through a LMCT transition and a subsequent Fenton reaction. Thus, the photoactive $[\text{FeOHCit}]^-$ complex and Fe^{3+} -siderophore complex (secreted by bacteria) undergoes a photolytic process whose primary step is a LMCT process with generate Fe^{2+} and ligand radical (Eqs. (8) and (9)) [43,44]. Fe^{2+} will undergo a Fenton reaction with added and formed hydrogen peroxide to produce HO^\bullet (Eq. (10)). The citrate ligand oxidized HGA^{2-} (3-hydroxyglutaric acid) in the presence

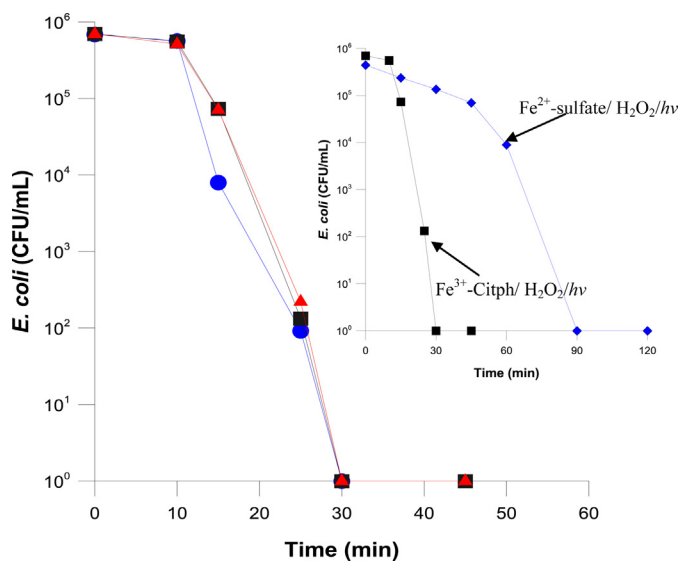


Fig. 5. $E. coli$ inactivation during photo-Fenton process mediated by Fe-citrate at different pH values: (\blacktriangle) pH 6.5; (\blacksquare) 7.5 and (\bullet) 8.5. Insert: comparison of the photo-Fenton treatment using FeSO_4 and Fe-citrate at pH 7.5. Fe^{2+} -citrate or FeSO_4 concentration: 0.6 mg/L relative to the Fe content, $[\text{H}_2\text{O}_2]$: 10 mg/L. Irradiated with simulated solar light. Experiments were conducted in triplicate and standard error was found to be approximately 5%. (For interpretation of the references to colour in this figure legend, the reader is referred to the web version of this article.)

of oxygen, result in superoxide radical anion ($\text{O}_2^\bullet^-$) that is in acid-base equilibrium with the hydroperoxyl radical (Eqs. (11) and (12)). These radicals can disproportionate to hydrogen peroxide (Eqs. (13) and (14)). It has been reported by speciation computations and kinetics experiments that Fe^{2+} and citrate complex react efficiently with H_2O_2 to produce HO^\bullet in aqueous solutions with pH ranging from 3 to 8 [14].

3.4. Effect of pH on bacterial inactivation rates during Fe-citrate-based photo-Fenton process

The influence of pH values of 6.5, 7.5 and 8.5 were evaluated on $E. coli$ inactivation by photo-Fenton reagent in the presence of H_2O_2 and Fe-citrate complex as iron source. Interestingly, in this pH range, the efficiency of the Fe-citrate-based photo-Fenton process to bacterial inactivation is independent of pH. Fig. 5 (traces (\blacktriangle), (\blacksquare) and (\bullet)) shows that the complete bacterial inactivation was achieved in all cases before 30 min of treatment, with very close inactivation rate constants (Table 2), at pH levels of 6.5, 7.5 and 8.5, respectively (Table 2). The bacterial inactivation rate was not correlated with the HO^\bullet production rate for the tested pH values (Fig. 4). Probably, in the full range of experimental conditions reported here, the HO^\bullet production rate was high enough to reach the maximum bacterial inactivation rate. In other words, the process was not limited by the HO^\bullet availability even at pH 6.5 and 7.5.

Dissolved iron was present during the entire Fe-citrate-mediated photo-Fenton reaction at pH 6.5 and 7.5 in the presence of bacteria (Table 2). In contrast, dissolved iron was not detected after 20 min of reaction at the same pH values in the absence of bacteria (Fig. 2b, traces (\blacktriangle) and (\blacksquare)). This could be explained by the siderophores secreted by $E. coli$ (e.g. ferritins and aerobactin) [45] that can chelate iron, allowing for its solubilization. The photo-reduction of Fe^{3+} from Fe^{3+} -siderophore complexes under UV-A and visible radiation produces HO^\bullet and regenerates Fe^{2+} via LMCT [43,44]. However, in the experiments conducted at pH 8.5, dissolved iron was negligible after 60 min of Fe-citrate-mediated photo-Fenton reaction in the presence of bacteria, even if the detec-

Table 2

Summary of inactivation rate constants K_{obs} [min^{-1}] obtained from fitting of plots of $\log (\text{CFU/mL})$ vs. time. Values of pH, dissolved Fe and H_2O_2 at the initial time (0 min) and final time (120 min) for all the experiments.

Systems	K_{obs} [min^{-1}]	pH		Fe (mg/L)			H_2O_2 (mg/L)	
		Initial	Final	0 min	60 min	120 min	Initial	Final
Fig. 5 Effect of the pH								
Fe–citrate + H_2O_2 + light	0.735 ± 0.003	6.5	5.4	0.6	0.3	0.2	10.0	2.8
Fe–citrate + H_2O_2 + light	0.754 ± 0.014	7.5	6.2	0.6	0.2	0.2	10.0	2.2
Fe–citrate + H_2O_2 + light	0.695 ± 0.009	8.5	7.5	0.6	0.1	N. D	10.0	1.5
FeSO ₄ + H_2O_2 + light	0.163 ± 0.021	7.5	6.8	N. D	N. D	N. D	10.0	7.4
Fig. 6								
Effect of the Fe–citrate concentration	0.287 ± 0.009	6.5	6.3	0.1	0.05	0.03	10.0	9.8
	0.485 ± 0.015	6.4	6.1	0.3	0.04	0.02	10.0	5.9
	0.736 ± 0.001	6.5	5.5	0.6	0.3	0.2	10.0	2.7
	0.737 ± 0.003	6.5	5.7	1.0	0.5	0.2	10.0	2.8
	0.751 ± 0.012	6.5	5.5	2.0	0.8	0.4	10.0	2.5
Fig. 7								
Fe–citrate + H_2O_2 + light	0.736 ± 0.001	6.5	5.4	0.6	0.3	0.2	10.0	2.8
FeSO ₄ + H_2O_2 + light	0.241 ± 0.002	6.5	5.8	0.3	0.2	N. D	10.0	5.0
Goethite + H_2O_2 + light	0.137 ± 0.016	6.5	6.2	N. D	N. D	N. D	10.0	8.8
Fe–citrate + light	–	6.5	6.3	0.6	0.4	0.4	–	–
Fe–citrate + H_2O_2 + dark	–	6.5	6.4	0.6	0.3	0.3	10.0	9.4
Fig. 9 Lake Geneva								
Fe–citrate + H_2O_2 + light	0.263 ± 0.012	8.3	8.2	0.6	0.4	0.2	10.0	2.0
Fe–citrate + light	–	8.3	8.3	0.6	0.4	0.4	–	–
Fe–citrate + H_2O_2 + dark	–	8.3	8.3	0.6	0.5	0.5	10.0	9.2
H_2O_2 + light	–	8.4	8.3	–	–	–	10.0	9.3
Light	–	8.5	8.4	–	–	–	–	–

tion limit of the employed ICP-MS spectrometry was of 0.2–0.9 $\mu\text{g/L}$ (Table 2). This could be due to the non-soluble crystalline forms of iron species formed at high pH, which are more stable, to be complexed by siderophores [46]. These results are in good agreement with those reported by Waite and Morel [47], who detected photo-reduced iron from amorphous Fe-hydroxides at pH 6.5, but not at pH 8.0. They proposed that a hydroxylated ferric surface species is the primary chromophore (light absorbing compound), analogous to the photo-reduction of Fe(OH)^{2+} , they also said that at pH 8 the Fe^{3+} surface complex was more strongly hydrolyzed and less prone to photo-reduction. However, in this study, *E. coli* inactivation was reached before 30 min of treatment when dissolved iron was still detected. Therefore, the photo-Fenton reaction carried out at near-neutral and alkaline pH using citrate as source of iron was mainly conducted by a homogeneous reaction. Control experiments conducted in the absence of the Fenton reagents at different pH values of 6.5, 7.5 and 8.5 showed that the survival of bacteria was unaffected for the tested pH values under dark.

The insert in Fig. 5 shows a comparison of *E. coli* inactivation during homogeneous and heterogeneous photo-Fenton reaction mediated by Fe–citrate and FeSO₄, respectively, at initial pH level of 7.5. In this latter condition, Fe^{2+} from FeSO₄ was instantaneously converted into solid iron oxides by O_2 and H_2O_2 (Table 2). In fact, goethite ($\alpha\text{-FeO(OH)}$) and/or lepidocrocite ($\gamma\text{-FeO(OH)}$), which have been reported to be formed by oxidation of Fe^{2+} in solution at neutral pH [10,48], are probably involved in the bacterial inactivation reached after 90 min of treatment (insert in Fig. 5). In contrast, the Fe–citrate-mediated photo-Fenton reaction showed a faster bacterial inactivation rate compared to FeSO₄ system, with corresponding inactivation rate constants of $0.754 \pm 0.014 \text{ min}^{-1}$ and $0.163 \pm 0.021 \text{ min}^{-1}$, respectively. This is due to the presence of dissolved iron ions in the Fe–citrate-based photo-Fenton treatment (Table 2). They contribute to the homogenous catalytic cycle, thus accelerating the decomposition of H_2O_2 , which, in turn, results in enhancement of HO^{\bullet} production (Eq. (10)). This observation was corroborated by the hydrogen peroxide consumption that was greater for the Fe–citrate-mediated photo-Fenton reaction (78%) than FeSO₄-mediated photo-Fenton reaction (26%) (Table 2).

The pH of the solutions decreases roughly by 1 unit for all the studied systems (Table 2). This concomitant decrease in pH is the result of aliphatic acids generated during photocatalytic oxidation of both bacteria and citrate ligands by HO^{\bullet} radical produced by photo-Fenton reaction. Previous studies have demonstrated that the pH value of Fe–citrate-mediated photo-Fenton reaction had a great effect on the degradation extend of organic compounds. Silva et al. [13] showed a decrease of herbicide degradation efficiency as the pH increase during iron–citrate-based photo-Fenton process under solar irradiation. However, in this study, the application of this complex towards inactivation of microorganisms present in aqueous solution was not significantly affected by pH. This remarkable finding indicates that, when using Fe–citrate as source of iron during photo-Fenton treatment, the bacterial inactivation can be carried out at near-neutral and alkaline pH, which is advantageous for environmental applications.

3.5. Influence of Fe–citrate concentration on bacterial inactivation by photo-Fenton processes

To inspect the effect of Fe–citrate concentration on *E. coli* inactivation, the experiments were conducted in the presence of 0.1, 0.3, 0.6, 1.0 and 2.0 mg/L of iron, with 10 mg/L H_2O_2 , at pH 6.5. Due to efficiency of the Fe–citrate-based photo-Fenton process to bacterial inactivation was independent of the pH in the range of 6.5 to 8.5 (Section 3.4), a value of 6.5 was selected for the evaluation of the others parameters on the inactivation. The results shown in Fig. 6 (traces (●), (▲) and (▲)) indicate that increasing the Fe–citrate concentration from 0.1 mg/L to 0.6 mg/L (concentrations relatives to the Fe content) has a positive effect on the rate of bacterial inactivation. The initial Fe–citrate concentration doses of 0.1 and 0.3 mg/L resulted in complete bacterial inactivation after 75 and 45 min of reaction, with inactivation rate constants of $0.287 \pm 0.001 \text{ min}^{-1}$ and $0.485 \pm 0.015 \text{ min}^{-1}$, respectively (Fig. 6, traces (●) and (▲)). When the Fe–citrate concentration was increased to 0.6 mg/L (concentration relative to the Fe content), the inactivation was improved with an inactivation rate constant of $0.736 \pm 0.001 \text{ min}^{-1}$ (Table 2). These results can be explained by an increase in the reaction kinetics due to the higher iron concentration [49,50].

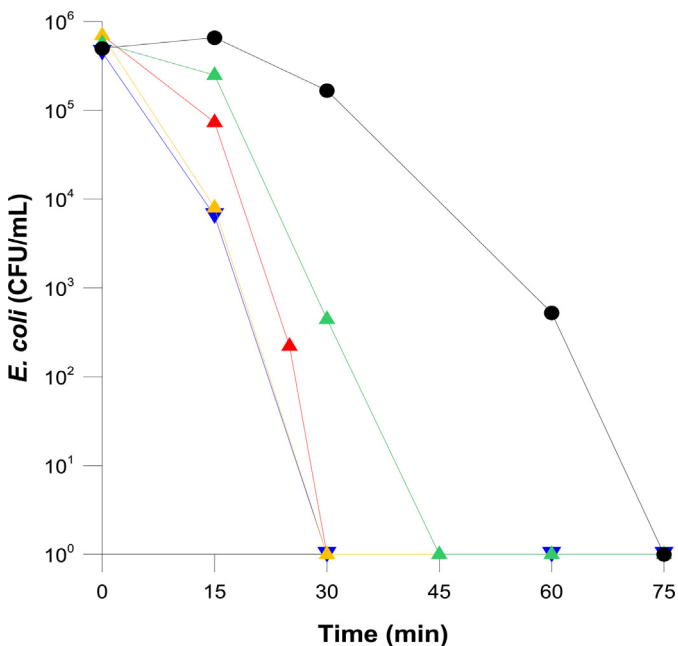


Fig. 6. *E. coli* inactivation during photo-Fenton process with different Fe-citrate concentrations: (●) 0.1 mg/L; (▲) 0.3 mg/L; (▲) 0.6 mg/L; (▼) 1.0 mg/L and (△) 2.0 mg/L. Concentrations relatives to the Fe content, [H₂O₂]: 10 mg/L, pH 6.5. Irradiated with simulated solar light. Experiments were conducted in triplicate and standard error was found to be approximately 5%. (For interpretation of the references to colour in this figure legend, the reader is referred to the web version of this article.)

which was also observed in a faster consumption of H₂O₂. This certainly promotes a higher generation of hydroxyl radicals and consequently, induces an enhancement of bacterial inactivation rate. Correspondingly, after 120 min of treatment, 2%, 41% and 73% of H₂O₂ were consumed for 0.1, 0.3 and 0.6 mg/L of iron, respectively (Table 2). Nevertheless, at higher concentrations of Fe-citrate (1.0 and 2.0 mg/L), no significant differences were found in the inactivation rate constants, compared with a concentration of 0.6 mg/L, k_{obs} were $0.737 \pm 0.003 \text{ min}^{-1}$, $0.751 \pm 0.012 \text{ min}^{-1}$ and $0.736 \pm 0.001 \text{ min}^{-1}$, respectively. As shown in Eqs. (8) and (10), a higher level of HO[•] radicals generation was expected at a higher Fe-citrate concentration due to the enhanced absorption of light by Fe-complexes [19]. However, photo-generated HO[•] radicals could react with both bacteria and Fe-citrate complex. Thus, when the concentration of Fe-citrate increased, the role of the Fe-citrate as a competitor for the HO[•] reaction could also be more important [18]. These results indicate that low ranges of concentration of Fe-citrate (Fe-citrate concentration: 0.6 mg/L relative to the Fe content) in homogeneous photo-Fenton system at near-neutral pH are adequate to efficiently inactivate *E. coli* under specific experimental conditions.

3.6. Bacterial inactivation by photo-Fenton process using different iron sources

The positive effect of the Fe-citrate complex was compared, in terms of bacterial inactivation efficiency, with the other sources or iron: cationic iron (FeSO₄) and goethite at pH 6.5. The benefit of using the iron-citrate complex, as iron source in the photo-Fenton process for the bacterial inactivation was clear, reaching total bacterial inactivation before 30 min of treatment, while for FeSO₄ and goethite-based photo-Fenton systems bacterial inactivation was reached before 90 min of treatment (Fig. 7, traces (▲), (◆) and (●)). The inactivation rate constants, presented in Table 2, confirmed the effects observed on the curves. The higher effi-

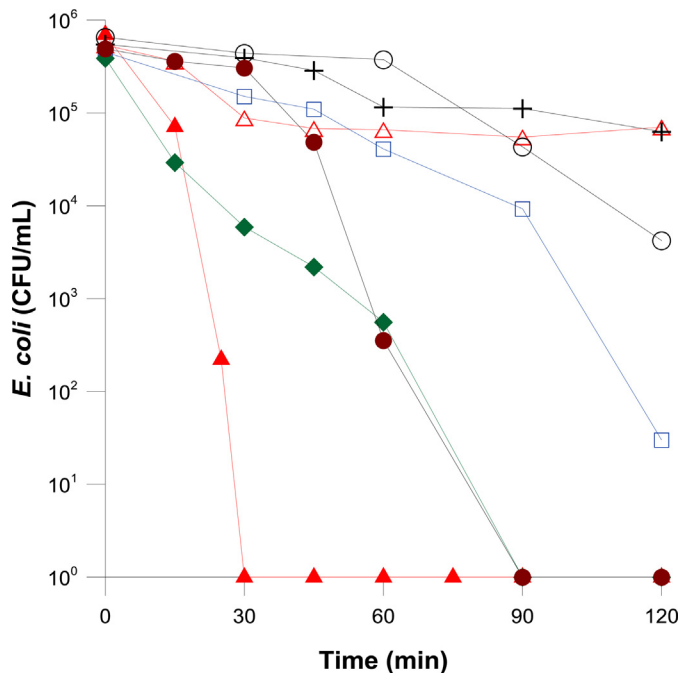


Fig. 7. *E. coli* inactivation during photo-Fenton process mediated by different iron sources. (▲) Fe-citrate/H₂O₂/light; (◆) FeSO₄/H₂O₂/light and (●) goethite/H₂O₂/light. Control experiments: (○) Fe-citrate/light; (+) Fe-citrate/H₂O₂/dark; (○) light alone; (□) H₂O₂/light. Fe-citrate or FeSO₄ or goethite concentration: 0.6 mg/L relative to the Fe content, [H₂O₂]: 10 mg/L, pH 6.5. Irradiated with simulated solar light. Experiments were conducted in triplicate and standard error was found to be approximately 5%. (For interpretation of the references to colour in this figure legend, the reader is referred to the web version of this article.)

ciency of bacterial inactivation observed with Fe-citrate complexes ($k_{\text{obs}} = 0.736 \pm 0.001 \text{ min}^{-1}$) in relation to cationic iron (FeSO₄) ($k_{\text{obs}} = 0.241 \pm 0.00 \text{ min}^{-1}$) or goethite ($k_{\text{obs}} = 0.137 \pm 0.007 \text{ min}^{-1}$) can be attributed to several reasons. First of all, the citrate forms stable complexes with Fe³⁺ and leads to the higher solubility and stabilization of iron in aqueous solution at neutral pH, which leads to higher activity of iron in solution. Dissolved iron was observed during entire treatment period (Table 2). Secondly, the photoactivity of the Fe-citrate species, which generates Fe²⁺ with a relatively high quantum yield ($\Phi_{\text{Fe}^{2+}}$) that improve the photo-Fenton reaction [36,37]. On the contrary, for the FeSO₄-based photo-Fenton systems, the dissolved iron passed from 0.4 mg/L to 0.2 mg/L after 60 min of reaction, suggesting a lesser contribution of a homogeneous photo-catalytic reaction than with Fe-citrate. Then, after 60 min of treatment, iron precipitates and a transition from a homogenous to a heterogeneous process occurred (Table 2). Thus, after 60 min of treatment *E. coli* inactivation was mediated by the heterogeneous photocatalytic action of solid iron species that participated in the (photo) Fenton reactions, although at slower rates than dissolved iron [51]. In our previous paper [10], it was shown that iron (hydr) oxide alone or mixed as goethite ($\alpha\text{-FeOOH}$) and lepidocrocite ($\gamma\text{-FeOOH}$) were formed by oxidation of Fe²⁺ in solution during photo-Fenton process at neutral pH. When goethite was used as source of iron in the photo-Fenton process, dissolved iron was not detected in the filtrate samples during the reaction (Table 2). Thus, *E. coli* inactivation was mediated by a heterogeneous photo-Fenton process from the beginning of the reaction.

The H₂O₂ consumption was related with the extent of dissolved iron for the three iron sources. 72%, 50% and 12% of H₂O₂ were consumed after 120 min of treatment in the presence of Fe-citrate, iron sulphate and goethite, respectively (Table 2). The higher H₂O₂ consumption in the presence of organic complexes is also related

to the higher quantum yield of Fe^{2+} generation as compared to cationic iron (FeSO_4) or goethite. The quantum yield, in moles of Fe^{2+} produced per photon of incident UV radiation, increases in the following order: Fe^{3+} -complexes > dissolved (Fe^{3+}) species > Fe^{3+} in oxide form [25,52]. The same results were observed for degradation of organic compounds [13,25,53] where a higher efficiency with iron citrate was found as compared to iron salt.

The inactivation of *E. coli* by a homogenous photo-Fenton process may be explained by:

- Internal process, where endogenous photo-sensitizers and internal iron sources synergistically coupled to external UV and Fenton reactants (Fe^{2+} , H_2O_2) lead to oxidative stress through the intracellular Fenton's reaction, generating highly toxic HO^\bullet that can directly attack DNA and other intracellular components leading to bacterial growth inhibition,
- Contribution of external pathways, where exogenous short-living reactive oxygen species (ROS) formed outside of the cell, such as singlet oxygen (${}^1\text{O}_2$), H_2O_2 and $\cdot\text{OH}$, directly attack the external cell membrane and initiate lipid peroxidation chain reactions. This increases membrane permeability and subsequently alters normal cell functions and affects cell viability [54]. However, we consider that the internal (photo) Fenton mechanism represents a key contribution to the overall inactivation process, since the photo-Fenton treatment at neutral pH induces only slight lipid peroxidation and cell permeability changes, as reported in our previous paper [6].

The mechanism involved in goethite-based heterogeneous photo Fenton process can be summarized by two mechanisms:

- Photo-reduction of $>\text{Fe}^{3+}\text{OH}$ to $>\text{Fe}^{2+}$ on the surface of iron-bearing particles, under Vis irradiation [55], which subsequently reacts with H_2O_2 generating HO^\bullet radicals at the particle surface. Then, the generated HO^\bullet radicals attacked the bacteria adsorbed on the surface of the iron oxide particles. ($>\text{Fe}^{3+}\text{OH}$ and $>\text{Fe}^{2+}$ represent the iron species in solid or solution phase),
- Photocatalytic action of goethite, which possesses semiconductor properties with a band gap of 2.0–2.3 eV, typical to iron oxide semiconductors. Electrons and hole that are photo-generated in the goethite particles are scavenged by surface sites ($>\text{FeOH}$) to produce HO^\bullet radicals and $>\text{Fe}^{2+}$. Also, conduction band electrons could react with O_2 to form $\text{O}_2^{\bullet-}$ and generate HO^\bullet by several subsequent steps [56]. Furthermore, the photo-generated holes in the valence-band of goethite can directly react with bacteria [10,56]. Therefore, the reactive HO^\bullet radicals formed during these processes at the goethite and/or from direct oxidation of bacteria by surface holes could contribute to achieving complete bacterial inactivation after 90 min of treatment for the goethite/ H_2O_2 /light system (Fig. 7, trace (●)).

To get a better insight into the Fe-citrate complex-mediated bacterial inactivation through the formation of hydroxyl radicals, we compared the HO^\bullet formation during the photo-Fenton process using different iron sources. The results shown in Fig. 8 indicate that HO^\bullet radicals were not detected before illumination. This finding suggests that exposure to the simulated solar light was essential for generation of ROS for the photo-Fenton process using different iron sources. From the results shown in Fig. 8 (traces (▲), (◆) and (●)) it can be seen that the trend of HO^\bullet radical formation agreed well with the trend of bacterial inactivation during photo-Fenton treatment with different iron sources (Fig. 7, traces (▲), (◆) and (●)). This indicates that the bacterial inactivation is due to the production of HO^\bullet and that Fe-citrate can enhance the HO^\bullet formation in

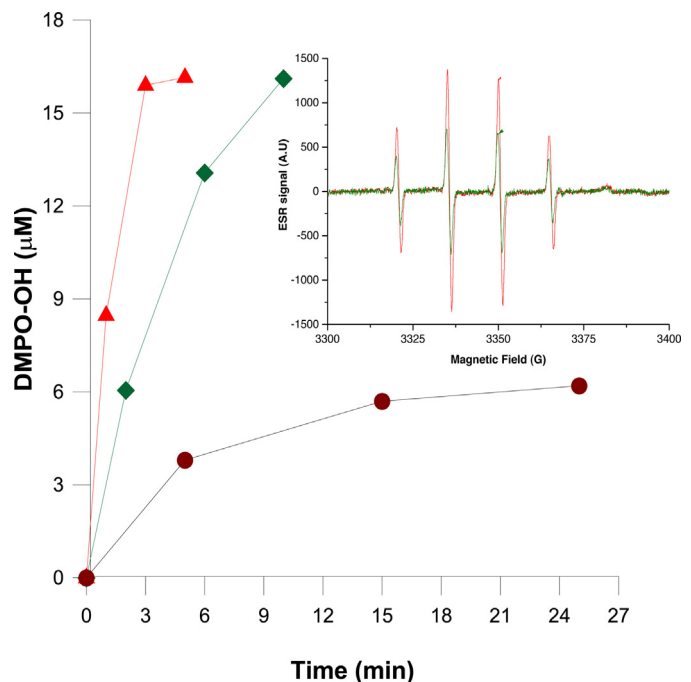


Fig. 8. The ESR-measured formation of hydroxyl radical (HO^\bullet) during photo-Fenton process mediated by different iron sources. (▲) Fe -citrate/ H_2O_2 /light; (◆) FeSO_4 / H_2O_2 /light and (●) goethite/ H_2O_2 /light. Concentration: 0.6 mg/L relative to the Fe content, $[\text{H}_2\text{O}_2]$: 10 mg/L, irradiated with simulated solar light. Insert: a typical ESR spectrum of the Fe -citrate/ H_2O_2 /light (red), FeSO_4 / H_2O_2 /light (green) systems. (For interpretation of the references to colour in this figure legend, the reader is referred to the web version of this article.)

the photo-Fenton process compared to FeSO_4 - and goethite-based photo-Fenton treatments. This result is consistent with previous findings, which suggested that HO^\bullet radical was the main species responsible for inactivating *E. coli* in the photoferrioxalate system under slightly acidic and near-neutral pH conditions 19.

The results of the photo-activity of Fe-citrate complex evaluated in absence of H_2O_2 are shown in Fig. 7. In particular, the trace (Δ) shows $1.0 \log_{10}$ reduction of the number of live bacteria during the first 30 min of treatment. This could be attributed to a combined action of $\text{HO}_2^\bullet/\text{O}_2^{\bullet-}$ radicals formed during the photo-reduction of Fe-citrate via reactions (Eqs. (11) and (12)). The photo-generation of $\text{O}_2^{\bullet-}$ from Fe-citrate solution was detected only qualitatively, by electron spin resonance spectroscopy (ESR) and was not sufficient for the quantitative analysis. Furthermore, the possibility of the involvement of a ligand radical, 3-hydroxyglutaric acid, (3-HGA^{2-}), in inactivating *E. coli* cannot be excluded. These radical species are generated in the photo-reduction of Fe-citrate, as highlighted in Eq. (8). Nevertheless, due to the instantaneous decarboxylation and oxidation of HGA^{2-} (Eq. (11)), the chance of inactivating *E. coli* by Citrate^{2-} is minimal. Beyond 30 min of treatment a plateau was observed (Fig. 7, traces (Δ)), possibly due to the Fe-citrate complex degradation. A similar result was observed by Cho et al. [19] who detected a slight photo-inactivation of *E. coli* for ferrioxalate complex in the absence of H_2O_2 dose at near-neutral pH. Fe-citrate complex absorbs in the UV and near-visible light (Fig. 1) producing a light screening effect, hindering its penetration in the water, and thus, protecting the bacteria. The negative screen effect was observed with regard to the control experiment under light alone (Fig. 7, traces (Δ) and (○)).

In the absence of light, the Fe-citrate/ H_2O_2 system (Fenton-like process) resulted in $0.5 \log_{10}$ reduction of *E. coli* inactivation during 60 min of reaction time (Fig. 7, trace (+)). The absence of light limits Fe^{2+} regeneration (Eqs. (8) and (9)), and the catalytic

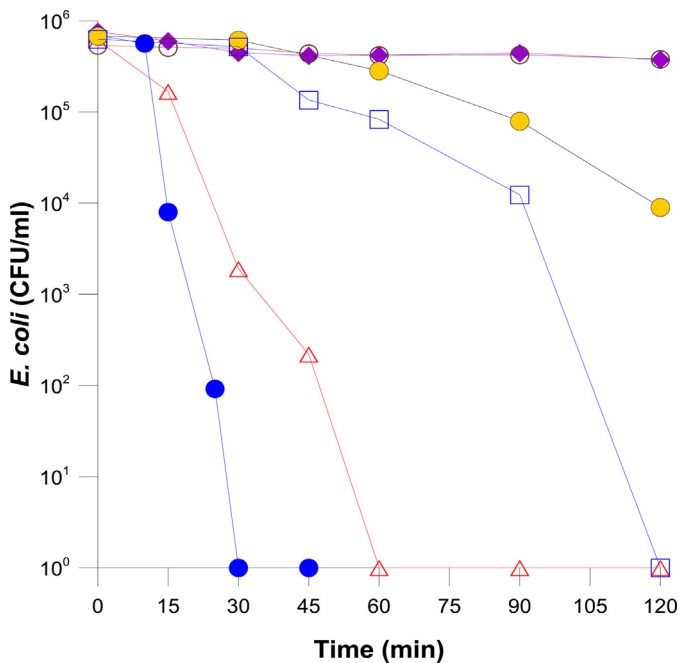


Fig. 9. *E. coli* inactivation during photo-Fenton process. *E. coli* were suspended in natural water and Milli-Q water having the characteristics described in Table 2. (◆) Fe-citrate/light, Lake water; (○) Fe-citrate/H₂O₂/dark, Lake water; (△) Fe-citrate/H₂O₂/light, Lake water (●) Fe-citrate/H₂O₂/light, Milli-Q water (pH 8.5); (□) H₂O₂/light; (●) light alone. Fe-citrate concentration: 0.6 mg/L relative to the Fe content, [H₂O₂]: 10 mg/L. Irradiated with simulated solar light. Experiments were conducted in triplicate and standard error was found to be approximately 5%. (For interpretation of the references to colour in this figure legend, the reader is referred to the web version of this article.)

cycle is, therefore, limited. Another control experiment under light alone (Fig. 7, trace (○)) shows that the sunlight affects bacteria, although not immediately. The curve has a shoulder, which corresponds to first resistance phenomenon due to the self-defence and auto-repair mechanisms of *E. coli* [57]. After that, the inactivation rate increases considerably reached 2 log reductions of bacteria at 420 min of treatment. It is the resulted from alteration in the bacterial metabolism through UV-A radiation. As the deleterious action of UV-A radiation was indirect, its effect on bacterial cultivability mainly resulted from photosensitization of endogenous chromophores such as co-enzymes or cytochromes, which could damage enzymes essential to bacteria growth [58].

3.7. Bacterial inactivation by Fe-citrate-based photo-Fenton process in natural water

In order to evaluate the effect of dissolved organic and mineral matter present in natural drinking water sources on the activity of Fe-citrate-based photo-Fenton process during bacterial inactivation, water samples originating from Lake Geneva were used and compared with Milli-Q water. As can be seen in Fig. 9 (traces (△) and (●)), for the Fe-citrate/H₂O₂/light system, at the pH of 8.5, a complete *E. coli* inactivation was achieved before 60 and 30 min of treatment in both natural and Milli-Q water, respectively. The inactivation rate constants presented in Table 2, confirm that the chemical components of the natural water do not enhance the Fe-citrate complex-mediated inactivation of bacteria through the homogeneous photo-Fenton action. Even if dissolved organic matter (DOM) had a positive effect on the complexation and solubilisation of iron resulting from photolysis of Fe-citrate complex [2] (Table 2), DOM can react with HO[•] and thus, disfavour the inactivation of bacteria. DOM substances can also absorb the UV-vis light

producing a light screening effect that limit the light absorption of the Fe-citrate to inactivate bacteria. Furthermore, the presence of bicarbonates ions in lake water (Table 2) probably affects the photo-Fenton system due to the scavenging the HO[•] radicals, since HCO₃⁻ react with HO[•] radicals to produce less reactive radicals, •CO₃⁻. The radical •CO₃⁻ is an electrophilic species reacting slower compared to •OH. Also, HCO₃⁻ absorbs light hindering its penetration in the water, thus protecting the bacteria [59]. Control experiments (Fe-citrate/H₂O₂) and (Fe-citrate/light), in natural water did not yield inactivation, indicating that neither homogeneous Fenton processes nor photo-reduction of Fe-citrate complex contributed to bacterial inactivation under our experimental conditions (Fig. 9, traces (+) and (△)). A negative screen effect was observed for Fe-citrate/light system, with regard to the control experiment under light alone, due to the absorption of Fe-citrate complex in the UV and near-visible light (Fig. 1), hindering its penetration in the water, thus, protecting the bacteria (Fig. 9, traces (◆) and (●)). For H₂O₂/light system control, complete bacterial inactivation was achieved before 120 min of treatment (Fig. 9, trace (□)).

The pH of the solution of Lake Geneva water remains constant during the treatment (the final pH was of 8.2, Table 2), thus, revealing a strong buffer capacity. This is due to the presence of carbonate, hydrocarbonate and phosphate ions in solution as shown in the composition of the natural water (Table 2). Instead, the pH in Milli-Q water for the system Fe-citrate/H₂O₂/simulated solar light decreased to the final pH value of 7.4. In each experiment, a residual peroxide concentration was detected at the end of the experiments ensuring the photo-Fenton reaction took place along of the treatment.

To be sure that the bacteria appearing as not-cultivable were inactivated, rather than slightly damaged, when using the photo-Fenton reaction, bacterial reactivation and/or growth of bacteria were verified. No bacterial reactivation and/or growth were observed at various pH values, different Fe-citrate concentrations and type of irradiations for the Fe-citrate-mediated photo-Fenton treatment (data not shown). The same results were observed when using samples of natural water. Furthermore, no bacterial reactivation and/or growth were observed when Fe-citrate, FeSO₄ and goethite were used as iron sources during the photo-Fenton process. This evidenced irreversible inactivation of bacteria by the homogenous photo-Fenton process at near-neutral and alkaline pH for all the iron sources and experimental conditions tested in this work.

4. Conclusions

Iron-citrate-mediated intensification of the solar photo-Fenton process showed promising results for bacterial inactivation at near-neutral and alkaline pH conditions, with using low iron concentration (Fe-citrate concentration: 0.6 mg/L relative to the Fe content) and avoiding precipitation of ferric hydroxides. Positive results were also obtained while applying this treatment for bacterial inactivation in natural water samples from Lake Geneva (Switzerland) at pH 8.5, since no bacterial reactivation and/or growth were observed after photo-Fenton treatment. This suggested irreversible inactivation, which is advantageous for environmental applications.

The homogeneous photo-Fenton process at near-neutral pH, with using Fe-citrate complex as a source of iron, markedly improved the efficiency of bacterial inactivation as compared to the heterogeneous photo-Fenton treatment (FeSO₄ and goethite as sources of iron). The bacterial inactivation rate increased in the order of goethite < FeSO₄ < Fe-citrate, which agreed well with the trend for the HO[•]radical formation. The key reason has been

attributed to the higher solubility and stabilization of iron in aqueous solution and a relatively high quantum yield of Fe–citrate complex.

This study reports the first application of Fe–citrate-based photo-Fenton chemistry for inactivation of *E. coli*. Another promising application of this system is related to the treatment of rural sites, where surface water or groundwater is frequently contaminated by agricultural chemicals and microorganisms. This type of application is promising, considering the simplicity of the installations and procedures, the possibility of using solar light, and safety of all chemicals employed in this system. Studies investigating larger-scale and field applications of the Fe–citrate-based photo-Fenton AOP are highly recommended.

Acknowledgements

The authors wish to thank the Swiss National Science Foundation for financial support through the program “Research partnership with developing countries” Project No. IZ70Z0.131312/1-2. We also thank Stefanos Giannakis for his contribution to the manuscript.

References

- [1] A. Safarzadeh-Amiri, J.R. Bolton, S.R. Cater, The use of iron in advanced oxidation processes, *J. Adv. Oxid. Technol.* 1 (1996) 18–26.
- [2] J.J. Pignatello, E. Oliveros, A. MacKay, Advanced oxidation processes for organic contaminant destruction based on the Fenton reaction and related chemistry, *Crit. Rev. Environ. Sci. Technol.* 36 (2006) 1–84.
- [3] A.G. Rincon, C. Pulgarin, Comparative evaluation of Fe³⁺ and TiO₂ photoassisted processes in solar photocatalytic disinfection of water, *Appl. Catal. B: Environ.* 63 (2006) 222–231.
- [4] J. Rodríguez-Chueca, M. Morales, R. Mosteo, M.P. Ormad, J.L. Ovelleiro, Inactivation of *Enterococcus faecalis*, *Pseudomonas aeruginosa* and *E. coli* present in treated urban wastewater by coagulation–flocculation and photo-Fenton processes, *Photochem. Photobiol. Sci.* 12 (2013) 864–871.
- [5] C. Ruales-Lonfat, A. Varón, J. Barona, A. Moncayo-Lasso, N. Benítez, C. Pulgarín, Iron-catalyzed low cost solar activated process for drinking water disinfection in Colombian rural areas, in: Technologies for Sustainable Development, Springer, 2013, pp. 1–16.
- [6] C. Ruales-Lonfat, N. Benítez, A. Sienkiewicz, C. Pulgarín, Deleterious effect of homogeneous and heterogeneous near-neutral photo-Fenton system on *E. coli*. Comparison with photo-catalytic action of TiO₂ during cell envelope disruption, *Appl. Catal. B: Environ.* 160–161 (2014) 286–297.
- [7] J. Rodríguez-Chueca, M.I. Polo-López, R. Mosteo, P. Fernández-Ibáñez, Disinfection of real and simulated urban wastewater effluents using a mild solar photo-Fenton, *Appl. Catal. B: Environ.* 150–151 (2014) 619–629.
- [8] E. Ortega-Gómez, M.M. Ballesteros Martín, B. Esteban García, J.A. Sánchez Pérez, P. Fernández Ibáñez, Solar photo-Fenton for water disinfection: an investigation of the competitive role of model organic matter for oxidative species, *Appl. Catal. B: Environ.* 148–149 (2014) 484–489.
- [9] E. Ortega-Gómez, B. Esteban García, M.M. Ballesteros Martín, P. Fernández Ibáñez, J.A. Sánchez Pérez, Inactivation of natural enteric bacteria in real municipal wastewater by solar photo-Fenton at neutral pH, *Water Res.* 63 (2014) 316–324.
- [10] C. Ruales-Lonfat, J.F. Barona, A. Sienkiewicz, M. Bensimon, J. Vélez-Colmenares, N. Benítez, C. Pulgarín, Iron oxides semiconductors are efficient for solar water disinfection: A comparison with photo-Fenton processes at neutral pH, *Appl. Catal. B: Environ.* 166–167 (2015) 497–508.
- [11] A.-G. Rincón, C. Pulgarin, Absence of *E. coli* regrowth after Fe³⁺ and TiO₂ solar photoassisted disinfection of water in CPC solar photoreactor, *Catal. Today* 124 (2007) 204–214.
- [12] B. Morgan, O. Lahav, The effect of pH on the kinetics of spontaneous Fe(II) oxidation by O₂ in aqueous solution – basic principles and a simple heuristic description, *Chemosphere* 68 (2007) 2080–2084.
- [13] M.R.A. Silva, A.G. Trovó, R.F.P. Nogueira, Degradation of the herbicide tebuthiuron using solar photo-Fenton process and ferric citrate complex at circumneutral pH, *J. Photochem. Photobiol. A: Chem.* 191 (2007) 187–192.
- [14] R.G. Zepp, B.C. Faust, J. Hoigne, Hydroxyl radical formation in aqueous reactions (pH 3–8) of iron(II) with hydrogen-peroxide – The photo-Fenton reaction, *Environ. Sci. Technol.* 26 (1992) 313–319.
- [15] S. Papoutsakis, F.F. Brites-Nóbrega, C. Pulgarin, S. Malato, Benefits and limitations of using Fe(III)-EDDS for the treatment of highly contaminated water at near-neutral pH, *J. Photochem. Photobiol. A: Chem.* (2015).
- [16] Y. Sun, J.J. Pignatello, Chemical treatment of pesticide wastes. Evaluation of iron(III) chelates for catalytic hydrogen peroxide oxidation of 2, 4-D at circumneutral pH, *J. Agric. Food Chem.* 40 (1992) 322–327.
- [17] B.C. Faust, R.G. Zepp, Photochemistry of aqueous iron(III)-polycarboxylate complexes: roles in the chemistry of atmospheric and surface waters, *Environ. Sci. Technol.* 27 (1993) 2517–2522.
- [18] M.E. Balmer, B. Sulzberger, Atrazine degradation in irradiated iron/oxalate systems: effects of pH and oxalate, *Environ. Sci. Technol.* 33 (1999) 2418–2424.
- [19] M. Cho, Y. Lee, H. Chung, J. Yoon, Inactivation of *E. coli* by photochemical reaction of ferrioxalate at slightly acidic and near-neutral pHs, *Appl. Environ. Microbiol.* 70 (2004) 1129–1134.
- [20] C. Liang, C.J. Bruell, M.C. Marley, K.L. Sperry, Persulfate oxidation for in situ remediation of TCE. II. Activated by chelated ferrous ion, *Chemosphere* 55 (2004) 1225–1233.
- [21] M. Sillanpää, K. Pirkanniemi, Recent developments in chelate degradation, *Environ. Technol.* 22 (2001) 791–801.
- [22] X. Feng, Z. Wang, Y. Chen, T. Tao, F. Wu, Y. Zuo, Effect of Fe(III)/citrate concentrations and ratio on the photoproduction of hydroxyl radicals: application on the degradation of diphenhydramine, *Ind. Eng. Chem. Res.* 51 (2012) 7007–7012.
- [23] H.B. Abrahamson, A.B. Rezvani, J.G. Brushmiller, Photochemical and spectroscopic studies of complexes, of iron(III) with citric acid and other carboxylic acids, *Inorg. Chim. Acta* 226 (1994) 117–127.
- [24] H. Katsumata, S. Kaneko, T. Suzuki, K. Ohta, Y. Yobiko, Photo-Fenton degradation of alachlor in the presence of citrate solution, *J. Photochem. Photobiol. A: Chem.* 180 (2006) 38–45.
- [25] A.G. Trovó, R.F.P. Nogueira, Diclofenac abatement using modified solar photo-Fenton process with ammonium iron(III) citrate, *J. Braz. Chem. Soc.* 22 (2011) 1033–1039.
- [26] Y. Sun, J.J. Pignatello, Activation of hydrogen peroxide by iron(III) chelates for abiotic degradation of herbicides and insecticides in water, *J. Agric. Food Chem.* 41 (1993) 308–312.
- [27] E. Antonini, H.-J. Vidic, in: O. e. d. p. y. marca (Ed.), *Complejo de hierro-citato, procedimiento para su fabricación y su aplicación farmacéutica*, Spanish, 1994, 2015.
- [28] McGuigan Joyce, Conroy Gillespie, M. Elmore, Solar disinfection of drinking water contained in transparent plastic bottles: characterizing the bacterial inactivation process, *J. Appl. Microbiol.* 84 (1998) 1138–1148.
- [29] A.H. Geeraerd, V.P. Valdravidis, J.F. Van Impe, GInaFIT, a freeware tool to assess non-log-linear microbial survivor curves, *Int. J. Food Microbiol.* 102 (2005) 95–105.
- [30] Y. Chen, Z. Liu, Z. Wang, M. Xue, X. Zhu, T. Tao, Photodegradation of propanolol by Fe(III)-citrate complexes: kinetics, mechanism and effect of environmental media, *J. Hazard. Mater.* 194 (2011) 202–208.
- [31] P. Vukosav, V. Tomišić, M. Mlakar, Iron(III)-complexes engaged in the biochemical processes in seawater. II. Voltammetry of Fe(III)-malate complexes in model aqueous solution, *Electroanalysis* 22 (2010) 2179–2186.
- [32] P. Vukosav, M. Mlakar, V. Tomišić, Revision of iron(III)-citrate speciation in aqueous solution. Voltammetric and spectrophotometric studies, *Anal. Chim. Acta* 745 (2012) 85–91.
- [33] L.-C. Königsberger, E. Königsberger, P.M. May, G.T. Hefta, Complexation of iron(III) and iron(II) by citrate. Implications for iron speciation in blood plasma, *J. Inorg. Biochem.* 78 (2000) 175–184.
- [34] B. Binder, Mixed-valence complexes of iron(III) with iron(II) and mixed-metal complexes of iron(III) with tin(II) in aqueous citrate media, *Inorg. Chem.* 10 (1971) 2146–2150.
- [35] F. Rey, E. Calle, J. Casado, Study of the effects of concentration and pH on the dissociation kinetics of Fe(II)-fulvic acid complexes, *Int. J. Chem. Kinet.* 30 (1998) 63–67.
- [36] G.S.R. Krishnamurti, P.M. Huang, Influence of citrate on the kinetics of Fe(II) oxidation and the formation of iron oxyhydroxides, *Clays Clay Miner.* 39 (1991) 28–34.
- [37] A.N. Pham, T.D. Waite, Oxygenation of Fe(II) in the presence of citrate in aqueous solutions at pH 6.0–8.0 and 25(C): interpretation from an Fe(II)/citrate speciation perspective, *J. Phys. Chem. A* 112 (2008) 643–651.
- [38] J.P. Jolivet, C. Chaneac, E. Tronc, Iron oxide chemistry. From molecular clusters to extended solid networks, *Chem. Commun. (Camb)* 338 (2004) 481–487.
- [39] O. Abida, M. Kolar, J. Jirkovsky, G. Mailhot, Degradation of 4-chlorophenol in aqueous solution photoinduced by Fe(III)-citrate complex, *Photochem. Photobiol. Sci.* 11 (2012) 794–802.
- [40] G.R. Buettner, R.P. Mason, Spin-trapping methods for detecting superoxide and hydroxyl free-radicals in-vitro and in-vivo, *Methods Enzymol.* 186 (1990) 127–133.
- [41] T.B. Field, J.L. McCourt, W.A.E. McBryde, Composition and stability of iron and copper citrate complexes in aqueous solution, *Can. J. Chem.* 52 (1974) 3119–3124.
- [42] C. Zhang, L. Wang, F. Wu, N. Deng, Quantitation of hydroxyl radicals from photolysis of Fe(III)-citrate complexes in aerobic water, *Environ. Sci. Pollut. Res. Int.* 13 (2006) 156–160 (5 pp).
- [43] H.G. Upritchard, J. Yang, P.J. Bremer, I.L. Lamont, A.J. McQuillan, Adsorption to metal oxides of the pseudomonas aeruginosa siderophore pyoverdine and implications for bacterial biofilm formation on metals, *Langmuir* 23 (2007) 7189–7195.
- [44] W. Köster, ABC transporter-mediated uptake of iron, siderophores, heme and vitamin B12, *Res. Microbiol.* 152 (2001) 291–301.
- [45] S.C. Andrews, A.K. Robinson, F. Rodriguez-Quinones, Bacterial iron homeostasis, *FEMS Microbiol. Rev.* 27 (2003) 215–237.

- [46] B. Sulzberger, H. Laubscher, Reactivity of various types of iron(III) (hydr) oxides towards light-induced dissolution, *Mar. Chem.* 50 (1995) 103–115.
- [47] T.D. Waite, F.M.M. Morel, Photoreductive dissolution of colloidal iron oxides in natural waters, *Environ. Sci. Technol.* 18 (1984) 860–868.
- [48] R.M. Cornell, U. Schwertmann, *Iron Oxides in the Laboratory: Preparation and Characterization*, 2015, ISBN: 3527296697.2000.
- [49] M. Pérez, F. Torrades, J.A. García-Hortal, X. Domènech, J. Peral, Removal of organic contaminants in paper pulp treatment effluents under Fenton and photo-Fenton conditions, *Appl. Catal. B: Environ.* 36 (2002) 63–74.
- [50] F. Herrera, C. Pulgarin, V. Nadtchenko, J. Kiwi, Accelerated photo-oxidation of concentrated p-coumaric acid in homogeneous solution. Mechanistic studies, intermediates and precursors formed in the dark, *Appl. Catal. B: Environ.* 17 (1998) 141–156.
- [51] R.M. Cornell, U. Schwertmann, *The iron oxides: Structure, properties, reactions, occurrence and uses*, British, 2003.
- [52] K.H. Tan, *Humic Matter in Soil and the Environment. Principles and Controversies*, Marcel Dekker, New York, NY, USA, 2003.
- [53] A.P.S. Batista, R.F.P. Nogueira, Parameters affecting sulfonamide photo-Fenton degradation – Iron complexation and substituent group, *J. Photochem. Photobiol. A: Chem.* 232 (2012) 8–13.
- [54] E. Cabiscol, J. Tamarit, J. Ros, Oxidative stress in bacteria and protein damage by reactive oxygen species, *Int. Microbiol.* 3 (2000) 3–8.
- [55] J.K. Leland, A.J. Bard, Photochemistry of colloidal semiconducting iron-oxide polymorphs, *J. Phys. Chem.* 91 (1987) 5076–5083.
- [56] J. Xu, N. Sahai, C.M. Eggleston, M.A.A. Schoonen, Reactive oxygen species at the oxide/water interface: Formation mechanisms and implications for prebiotic chemistry and the origin of life, *Earth Planet. Sci. Lett.* 363 (2013) 156–167.
- [57] S. Helali, M.I. Polo-López, P. Fernández-Ibáñez, B. Ohtani, F. Amano, S. Malato, C. Guillard, Solar photocatalysis: a green technology for *E. coli* contaminated water disinfection. Effect of concentration and different types of suspended catalyst, *J. Photochem. Photobiol. A: Chem.* 276 (2014) 31–40.
- [58] S. Pigeot-Rémy, F. Simonet, D. Atlan, J.C. Lazzaroni, C. Guillard, Bactericidal efficiency and mode of action: a comparative study of photochemistry and photocatalysis, *Water Res.* 46 (2012) 3208–3218.
- [59] D. Rubio, E. Nebot, J.F. Casanueva, C. Pulgarin, Comparative effect of simulated solar light, UV UV/H₂O₂ and photo-Fenton treatment (UV-vis/H₂O₂/Fe²⁺, 3+) in the *E. coli* inactivation in artificial seawater, *Water Res.* 47 (2013) 6367–6379.